P-ISSN: 2798-1134 | E-ISSN: 2797-3549 | DOI: 10.52562/injoes.2024.998

Indonesian Journal of Earth Sciences

https://journal.moripublishing.com/index.php/injoes

| Research Article |

Subsurface Corrosivity Assessment Using Subsoil Resistivity in a Typical Basement Terrain: A Case Study of the Adebowale Area in Akure, Southwestern Nigeria

Igbagbo Adedotun Adeyemo*, Fuad Olamilekan Korode, Opeyemi Abiodun Olaniyan, Oluseye Emmanuel Faleye

Department of Applied Geophysics, Federal University of Technology, Akure, Nigeria
** Correspondence: aadeyemo@futa.edu.ng*

Received: 26 March 2024 / Accepted: 24 May 2024 / Published: 31 May 2024

Abstract: The aim of this study is to investigate and map the subsurface corrosivity of soils at various depths (0.5 - 3.0 m) within the Adebowale community in Akure, Southwestern Nigeria, and to identify safe zones for the burial of metallic objects based on soil resistivity measurements. Sixty vertical electrical sounding (VES) data points were acquired using the Schlumberger electrode array with half-current (AB/2) spacing ranging from 1 - 150/225 m. The VES survey delineated 3 - 5 subsurface layers across the study area, corresponding to topsoil, weathered layer, partially weathered basement, fractured basement, and fresh basement. Maps of longitudinal conductance, longitudinal resistivity, and iso-resistivity depth slices (0.5, 0.75, 1.0, and 3.0 m) were generated. The corrosivity of the subsoil in the study area was categorized into five types: very high corrosivity (< 50 Ωm), high corrosivity (50 - 100 Ωm), moderate corrosivity (100 - 150 Ωm), low corrosivity (150 - 200 Ωm), and negligible corrosivity (> 200 Ωm). At 1.0 m and 3.0 m depth surfaces, the areas of negligible to low corrosivity are about 70% and 85%, respectively, suggesting that corrosivity decreases with depth within the shallow subsurface of the study area. The longitudinal conductance and longitudinal resistivity maps of Adebowale indicated that the areas of negligible to low corrosivity are about 85% and 75%, respectively, corroborating the depth slice resistivity maps. In these areas, buried metallic utilities are safe; conversely, any metallic utilities buried within the moderate to very high corrosivity zones of the study area must be adequately protected to avoid corrosion.

Keywords: Subsoil, resistivity, depth slice, corrosivity

INTRODUCTION

Corrosion applies to any process that involves the degradation of metallic elements. It is a natural process that converts a refined metal to a more chemically stable form, such as its oxide, hydroxide, or sulfide (Beavers & Thompson, 2006). Corrosion results in the gradual destruction of metallic materials by chemical and electrochemical reactions with their environment (Najjaran et al., 2004). The best-known case is rust formation involving steel. This process is typically electrochemical, resembling the characteristics of a battery. When metal atoms are exposed to an environment containing water, they can produce electrons. This action can be confined locally to create a crack or pit, which could extend further, leading to general wastage. Soil parameters known to have the greatest influence on corrosion rates include moisture content, degree of aeration, pH, redox potential, resistivity, chloride concentration, mineralogical reactions, microbial presence, soil types, and temperature (Palmer, 1989; Picozzi et al., 1993).

The assessment of the regional corrosivity of subsurface environments is crucial for understanding the potential impact on infrastructure and environmental systems within a community. Soil resistivity, the property of soil that resists the flow of electric current, determines the flow of electric current that promotes corrosion in pipes. Soil resistivity varies with depth due to changes in soil composition, moisture content, and temperature. The higher the soil resistivity, the lower the risk of corrosion. Sandy soils are high on the resistivity scale and are therefore considered the least corrosive. Clay soils, especially those contaminated with saline water, are lowest on the same scale. Therefore, soil resistivity measurement is imperative in investigating the external corrosion of buried pipelines (Rim-rukch, 2006; Hussain & Tarig, 2014). Buried pipes are prone to corrosion under certain soil conditions below the earth's surface.

External corrosion of earth-buried pipelines has been linked to soil resistivity, which gives a better prediction of soil corrosiveness than any other soil properties (Romer et al., 2005).

Previous studies have extensively examined the corrosion rates of steel and their interactions with various soil parameters (Palmer, 1989; Picozzi et al., 1993; Romer et al., 2005; Rim-rukch, 2006; Bayowa & Adigun, 2012; Adeoti et al., 2013; Hussain & Tarig, 2014; Ngah & Abam, 2014; Alagbe, 2018; Adeyemo et al., 2018; Adeyemo et al., 2019; Akintunde & Ozebo, 2022; Eyankware & Umayah, 2022). Notably, Palmer (1989) and Picozzi et al. (1993) highlighted the significant influence of soil resistivity on corrosion processes, which directly informs our investigation of subsurface corrosivity using soil resistivity measurements in the Adebowale community. These studies provide a foundational understanding that helps us explore the specific geoelectric characteristics and corrosivity zones in our study area.

Dayal et al. (1988) consider soil resistivity to be the best criterion for estimating the corrosion of a given soil in the laboratory, where the vital parameter of moisture can be controlled. Braford (2000) considers soil resistivity the most commonly used indicator of soil corrosivity, while Hussain & Tarig (2014) observed that the use of resistivity to identify corrosion rates depends on the current flow between buried metallic utilities and the host subsoil.

Idornigie et al. (2006), on the basis of resistivity contrast, classified the subsoil of Akungba-Akoko, Ondo State, Nigeria, into four corrosivity zones: very strongly corrosive (less than 10 Ωm), moderately corrosive (10 - 60 Ωm), slightly corrosive (60 - 180 Ωm), and non-corrosive (180 Ωm and above). Guma et al. (2015) also undertook a study on the soil corrosivity level of the Kaduna metropolitan area using the electrical resistivity method. In terms of soil corrosivity rating, the study area was described as mildly corrosive on average, varying from aggressive at depths of less than about 0.5 m to slightly corrosive around 4.5 m depth. Bayowa & Olayiwola (2015) investigated the application of electrical resistivity on topsoil thickness, competence, and corrosivity to determine the suitability of soils in the study area for construction of buildings. Their results showed that the topsoil quality varied from highly competent (>750 Ωm) to moderately competent (107 - 347 Ωm), while soil corrosivity ranged between non-corrosive soils (200 Ωm) and mildly corrosive soil (100 - 200 Ωm). The study concluded that the study area is underlain by highly competent to competent and practically non-corrosive to mildly corrosive soils.

Despite numerous studies on soil corrosivity and steel interactions, there are no specific investigations into the subsurface corrosivity of soils in the Adebowale community using detailed geoelectric parameters. This study aims to fill this gap by adopting the Electrical Resistivity method to characterize the subsoil layers and identify distinct corrosivity zones within this specific region. Therefore, this study aims to determine the geoelectric parameters of subsoil layers in the Adebowale community, Akure, Southwestern Nigeria, and to classify the area into different corrosive zones at different depths (0.5 - 3.0 m). This will address the need for precise subsurface corrosivity assessment to guide infrastructure development and maintenance in the region.

To achieve the aim of this study, the specific objectives are to determine the geoelectric parameters of subsoil layers in the Adebowale community, identify specific depth slices or surfaces, characterize the subsurface layers into distinct corrosivity zones, and assess the implications of these corrosivity zones for infrastructure development and maintenance.

Description of the Study area

The study area, Adebowale community, is located along the Ondo-Akure Expressway after Owena Army Cantonment in the Ita-Oniyan area of Akure, Ondo State, Southwestern Nigeria. Adebowale community is situated in the South Western Basement Complex of Nigeria. Its geographical coordinates fall within 734163 - 736175 m (Easting) and 802200 - 803421 m (Northing), as shown in Figure 1.

The study area is easily accessible through a major tarred road and several untarred roads. The terrain is moderately to highly undulating with surface elevations ranging from 320 to 395 m above sea level (Figure 2). The climate is hot and humid, typical of the rainforest region of southwestern Nigeria. The rainy season lasts from April to October, with an annual rainfall of about 152 mm (Iloeje, 1980). The average temperature of the area is about 27°C during harmattan (December - February) and 32°C in March, with a mean annual relative humidity of about 80% (Iloeje, 1980; Adeyemo et al., 2023). The natural vegetation is tropical rainforest (Iloeje, 1980; Adeyemo et al., 2023). The area is underlain by Migmatite-Gneiss-Quartzite Complex rocks (Oyawoye, 1964; Rahman, 1976; Rahaman, 1989). The northern part of the area is predominantly quartzite, while migmatite-gneiss rocks dominate the southern part (Figure 3).

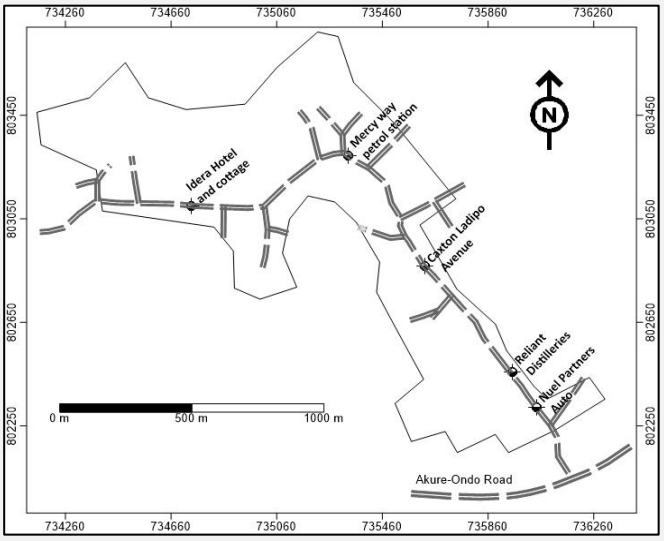

Figure 1. Layout map of the study area.

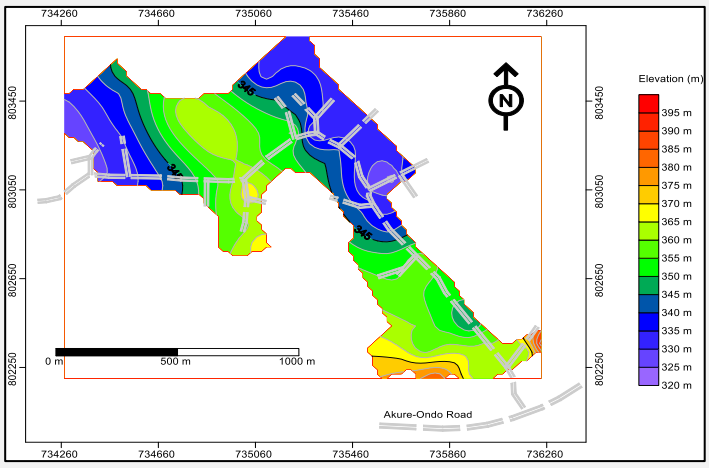

Figure 2. Topographic map of the study area.

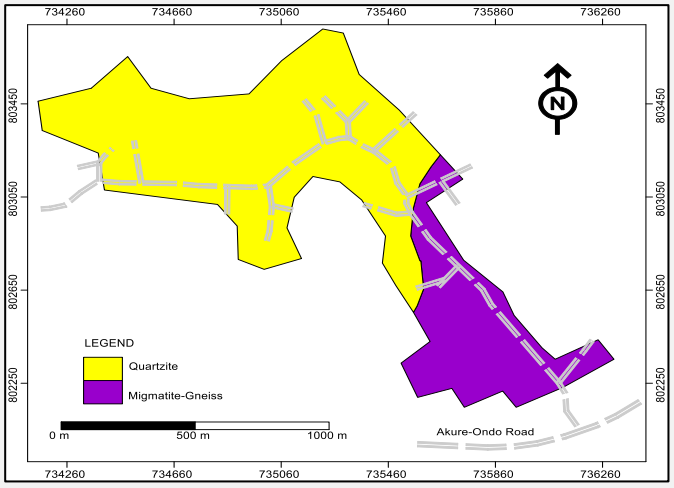

Figure 3. Simplify geological map of the study area.

MATERIALS & METHODS

The Omega Resistivity meter was used for data acquisition. Vertical Electrical Sounding (VES) was adopted for this work, as it allows measurement of soil resistivity at different depths and facilitates soil resistivity depth slicing (Kosinski & Kelly, 1981; Adeyemo et al., 2018; Adeyemo et al., 2019). VES data were acquired using the Schlumberger electrode configuration with a maximum half-current electrode separation (AB/2) of 150 - 225 m (Figure 4).

The vertical resistivity is measured with respect to a fixed center. To acquire this, potential differences are measured at different positions of the current electrode with respect to the fixed center, which is the station position. As the electrode separation increases, the potential difference values start decreasing. This reducing potential difference is compensated for by increasing the potential electrodes' separation. The apparent resistivity values of the successive layers are calculated using the general equations of the Schlumberger array (Equations 1-3).

$$\rho_{Schlumberger} = 2\pi R\left[\frac{L^2 - l^2}{4l}\right] \quad (1)$$

When L>>>/i.e. $L^2 - l^2 \approx L^2$. Such that:

$$\rho_a = \frac{\pi R L^2}{2l} \quad (2)$$

Equation 2 can also be written as:

$$\rho_a = \frac{\pi R \left(AB/2\right)^2}{MN} \quad (3)$$

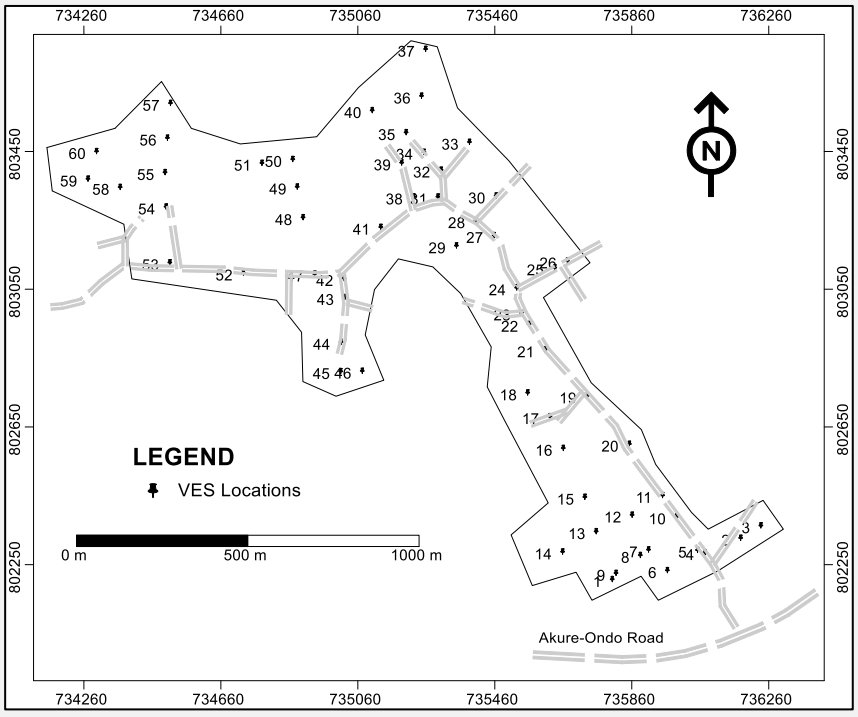

Figure 4. Base map showing VES locations.

The apparent resistivity(ρ_a) values were subsequently plotted on bilogarithmic paper as VES curves and then interpreted using the conventional manual curve matching technique (Keller & Frischknecht, 1966; Koefeod, 1979). The interpreted results were iterated using WinResist, a 1-D forward modeling software (Vander Velpen, 2004). The iterated results were presented in Table 1. The results were also presented as maps of longitudinal conductance, longitudinal resistivity, and iso-resistivity at different depth slices (0.5, 0.75, 1.0, 1.5, and 3.0 m). In all the resistivity maps, the study area was characterized into different corrosivity zones based on Gopal's (2010) classification (Table 2).

Second-order geoelectric parameters, including longitudinal conductance and longitudinal resistivity, were also determined to estimate the average conductance and resistivity values of the overburden materials in the area. The equations for determining the longitudinal conductance and longitudinal resistivity values are provided in Equations 4 and 5.

Longitudinal conductance (S)

$$S = \sum \frac{h_i}{\rho_i} = \frac{h_1}{\rho_1} + \frac{h_2}{\rho_2} + \frac{h_3}{\rho_3} + \cdots \frac{h_n}{\rho_n}$$ [Zohdy et al., 1974; Kosinski & Kelly, 1981] (4)

Where h_i is layer thickness; ρ_i is layer resistivity.

Longitudinal resistivity (ρ_L)

$$\rho_L = \frac{H}{S}$$ [Zohdy et al., 1974; Kosinski & Kelly, 1981] (5)

Where H is total overburden thickness; S is longitudinal conductance value.

RESULTS & DISCUSSION

The VES results are presented in Table 1 and several maps. The VES results delineated three to five geoelectric layers across the study area. Seven different sounding curve types were identified in the area: A, H, KH, K, HKH, HA, and AKH (Table 1). The resistivity of the topsoil, clayey sand weathered layer, sandy clay weathered layer, and weathered bedrock/fresh bedrock varies from 24 - 961 Ωm, 13 - 4141 Ωm, 24 - 72739 Ωm, and 122 - 100000 Ωm, respectively.

The subsurface geoelectric layers reflect different subsurface layers based on their resistivity contrast, which can be used to characterize the area into different corrosivity zones.

Table 1. The VES Summary Results

VES No	Easting (m)	Northing (m)	Resistivity ρ1/ρ2/…/ρn (Ωm)	Thickness h1/h2/…/hn (m)	Thickness
1	735803	802200	24/167/16130	3.3/1.8	A
2	736178	802320	87/814/1861	4.3/19.9	A
3	736237	802356	78/77/2023	1.9/2.1	H
4	736074	802278	41/576/3699	8.5/10.8	A
5	736052	802285	79/415/8238	5.6/62.2	A
6	735964	802226	69/188/3093	12.5/7.1	A
7	735909	802286	76/255/2167	3.8/12.4	A
8	735885	802270	46/73/633	2.7/1.4	A
9	735814	802218	69/1260/34408	6.8/16.4	A
10	735991	802382	68/587/4828	5.9/10.2	A
11	735950	802444	75/332/3097	1.2/16.3	A
12	735861	802387	88/368/250/786	0.6/2.0/13.8	KH
13	735756	802339	68/2521/407/7192	0.4/0.6/23.2	KH
14	735658	802280	136/4141/113/4360	1.9/3.3/12.1	KH
15	735723	802439	183/2675/380/61994	2.2/1/1/38.0	KH
16	735660	802581	328/40/590/132/14465	0.4/0.7/0.8/56.8	HKH
17	735621	802673	227/121/36742	0.4/34.7	H
18	735556	802742	88/796/24/11995	1.8/2.4/10.5	KH
19	735730	802733	129/156/39255	0.3/12.3	K
20	735853	802593	112/13/562	1.3/1.3	H
21	735607	802867	57/15/88/100000	1.9/1.9/1.7	HA
22	735560	802941	79/125/72739	1.5/5.0	A
23	735538	802974	31/2665/25/38127	0.4/0.8/2.1	KH
24	735524	803047	232/1650/115/4245	0.8/2.7/11.2	KH
25	735635	803105	56/145/3583	4.0/13.7	A
26	735672	803125	57/2010/96	0.8/0.9/8.2	KH
27	735458	803199	89/1412/246	0.7/1.2/17.2	KH
28	735405	803242	281/2171/139/5396	2.3/2.9/12.3	KH
29	735348	803169	150/1099/280/1758	1.5/3.1/21.1	KH

VES No	Easting (m)	Northing (m)	Resistivity ρ1/ρ2/…/ρn (Ωm)	Thickness h1/h2/…/hn (m)	Thickness
30	735464	803314	252/472/108/10948	1.0/4.3/20.9	KH
31	735294	803311	57/1480/50/92504	0.4/1.0/5.0	KH
32	735303	803389	67/321/319/9092	1.3/0.3/43.2	A
33	735386	803470	102/164/3502	1.0/30.2	A
34	735253	803441	157/250/792	1.0/31.2	A
35	735201	803498	168/391/2877/178/23084	0.5/4.1/6.3/31.6	AKH
36	735246	803604	59/295/493/34188	0.5/1.2/48.9	A
37	735258	803740	177/373/154/2018	1.0/2.1/20.3	KH
38	735223	803311	154/2210/128/2582	2.6/3.1/8.9	KH
39	735188	803410	48/1058/1154/122/100000	0.9/1.9/3.6/10.2	AKH
40	735102	803562	113/849/220/2019	0.9/0.8/4.4	KH
41	735127	803223	162/339/1454	4.6/0.7	A
42	735020	803074	194/38/447/188/3186	0.6/0.4/6.2/18.1	HKH
43	735022	803019	249/268/2019	1.1/9.5	A
44	735011	802889	156/578/4597	1.2/8.2	A
45	735010	802804	271/42/1343/100000	0.3/0.8/24.7	HA
46	735073	802805	52/2725/458/4149	0.7/1.2/70.4	KH
47	734934	803087	282/307/1060	2.3/6.6	A
48	734900	803251	192/2994/2725	1.7/7.2/34.1	KH
49	734883	803340	252/419/27272	3.1/13.8	A
50	734870	803420	35/1110/1433	1.1/27.4	A
51	734780	803409	961/466/44984	12.8/9.6	H
52	734726	803090	283/3439/538/6139	0.8/1.6/29.3	KH
53	734511	803120	88/382/119/20431	1.3/7.4/6.9	KH
54	734500	803282	89/1328/1456	1.7/76.7	A
55	734497	803382	131/660/6388	2.3/38.1	A
56	734504	803482	358/2067/2858	3.9/23.7	A
57	734513	803583	79/1897/169/76994	2.0/4.0/16.5	KH
58	734366	803339	56/258/17610	0.9/12.6	A
59	734272	803363	99/681/70955	1.0/49.3	A
60	734297	803443	81/622/10737	1.4/35.6	A

Table 2. Classification of soil corrosiveness from soil resistivity (Gopal, 2010)

Resistivity (Ωm)	Corrosive Probability
>200	Negligible
100 - 200	Low
50 - 100	High
<50	Very High

0.5 m Iso-Resistivity Depth Slice Map

The 0.5 m iso-resistivity depth slice map (Figure 5) reveals that a larger section (about 35%) of the area, consisting of the northwestern and a major segment of the southern parts, has very high resistivity (above 200 Ωm) and high resistivity (150 - 200 Ωm), suggesting negligible and low corrosivity, respectively. The northeastern part and a larger segment of the southern part of the area can be characterized as moderate (100 - 150 Ωm) to high (50 - 100 Ωm) corrosivity zones. At this depth (0.5 m), only parts of the study area considered to be in negligible and low corrosivity zones are suitable for burying metallic utilities without fear of corrosion.

0.75 m Iso-Resistivity Depth Slice Map

The 0.75 m iso-resistivity depth slice map (Figure 6) reveals that larger sections of the northwestern, central, and a major segment of the southern parts of the study area have very high resistivity (above 200 Ωm) and high resistivity (150 - 200 Ωm), suggesting negligible and low corrosivity, respectively. The northeastern part and a larger segment of the southern part of the area can be characterized as moderate (100 - 150 Ωm) to high (50 - 100 Ωm) corrosivity zones. At this depth (0.75

m), about 40% of the area can be classified as having negligible to low corrosivity. Only these parts of the area are suitable for burying metallic utilities without fear of corrosion.

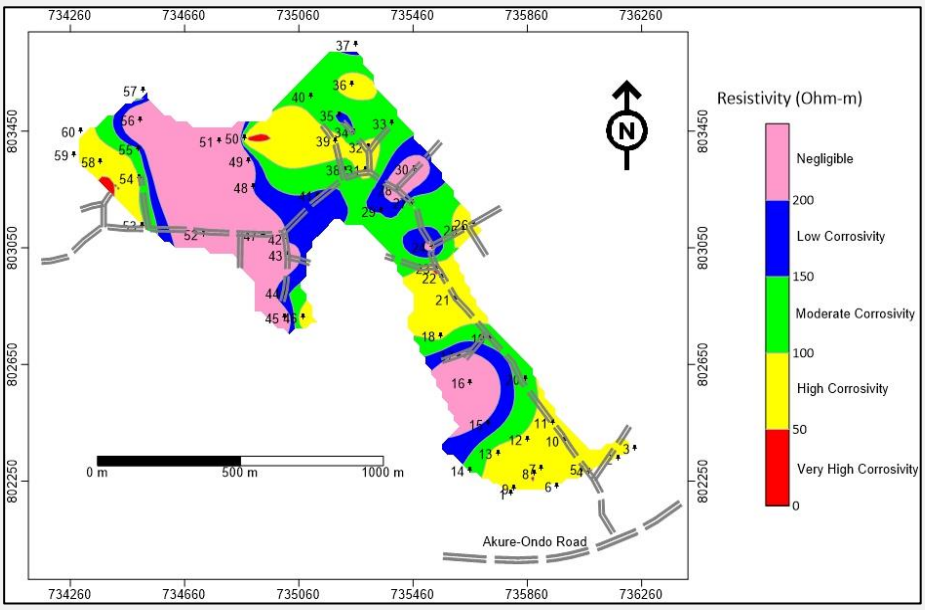

Figure 5. 0.5 m iso-resistivity depth slice map of the area.

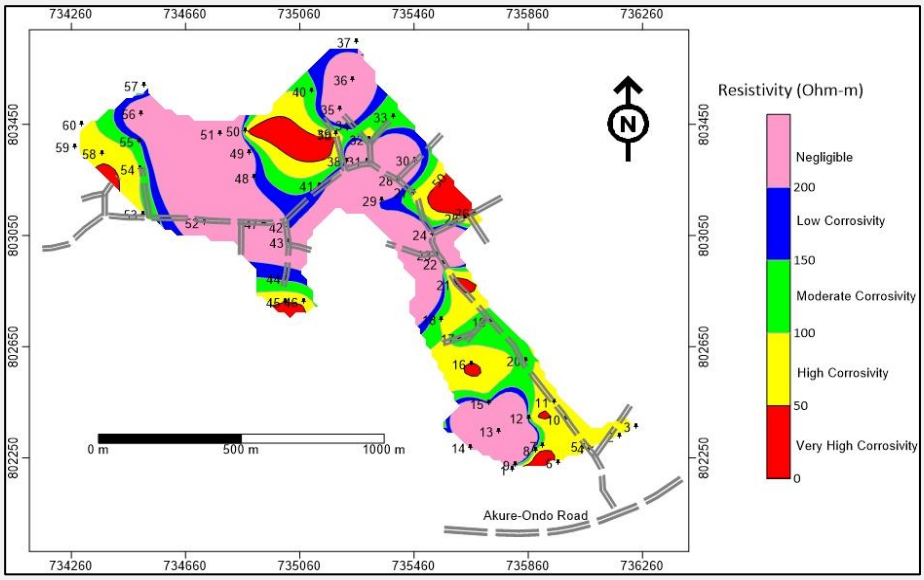

Figure 6. 0.75 m iso-resistivity depth slice map of the area.

1.0 m Iso-Resistivity Depth Slice Map

The 1.0 m iso-resistivity depth slice map (Figure 7) reveals that about 70% of the study area, encompassing the northwestern, central, and southern parts, has very high resistivity (above 200 Ωm) and high resistivity (150 - 200 Ωm), suggesting negligible and low corrosivity, respectively. About 5% of the study area, consisting of the north-central and extreme northwestern parts, exhibits moderate (100 - 150 Ωm), high (50 - 100 Ωm), and very high (0 - 50 Ωm) corrosivity.

3.0 m Iso-Resistivity Depth Slice Map

The 3.0 m iso-resistivity depth slice map (Figure 8) reveals that about 85% of the study area, covering the northwestern, northeastern, central, and larger parts of the southern regions, has very high

resistivity (above 200 Ωm) and high resistivity (150 - 200 Ωm), suggesting negligible and low corrosivity, respectively. The remaining 15% of the area shows moderate (100 - 150 Ωm), high (50 - 100 Ωm), and very high (0 - 50 Ωm) corrosivity.

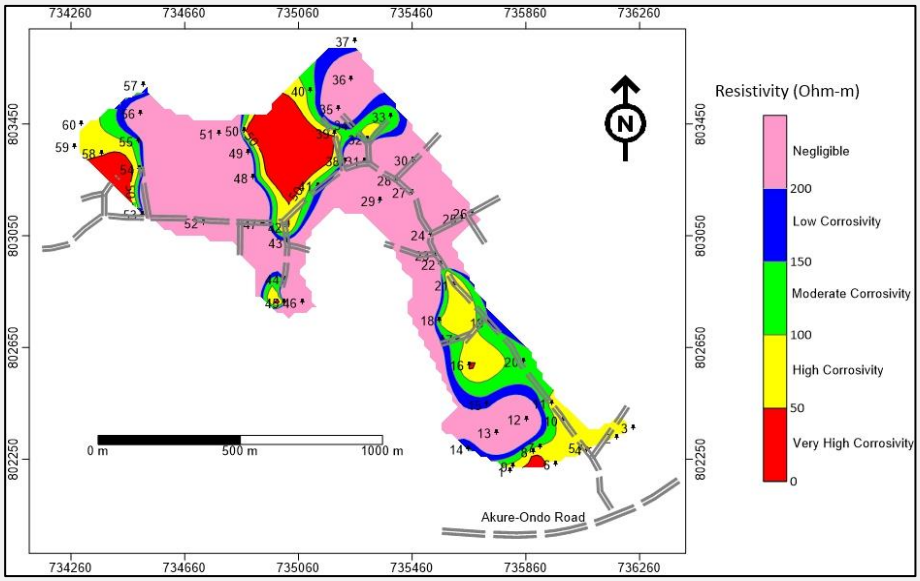

Figure 7. 1.0 m iso-resistivity depth slice map of the area.

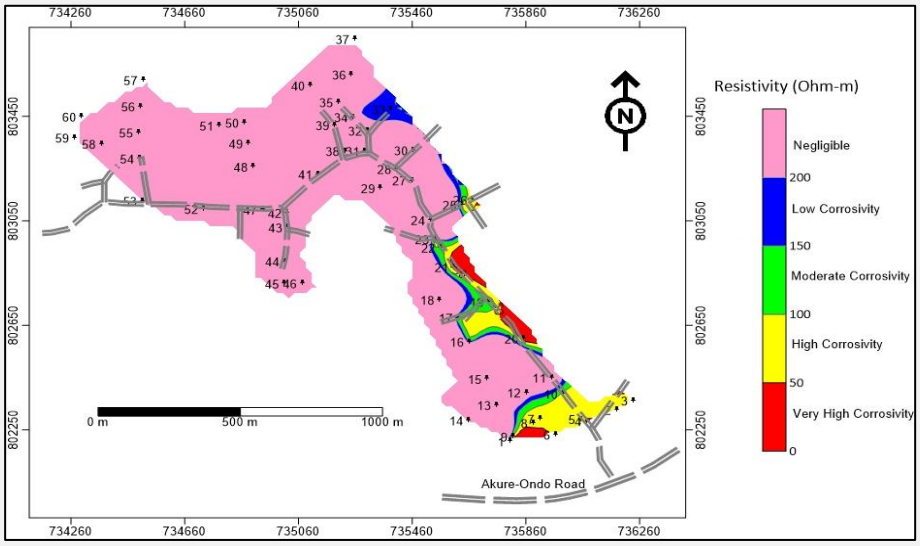

Figure 8. 3.0 m iso-resistivity depth slice map of the area.

Longitudinal Conductance Map

Longitudinal conductance is a measure of how easily electrical current can pass through subsoil material, and it is directly related to salinity, moisture, and clay content of the soil. Salinity and moisture content are key factors in determining soil corrosivity (Palmer, 1989; Picozzi et al., 1993). Generally, higher salinity, moisture, and clay contents lead to higher conductivity, indicating high corrosivity, while areas with low longitudinal conductance indicate a low risk of corrosivity. The longitudinal conductance map (Figure 9) indicates that a predominant portion of the study area (about 60%), notably the northwestern part, is characterized by very low longitudinal conductance (0.02 - 0.1 mhos), suggesting negligible corrosivity. About 25% of the area, notably in the northeastern region, is characterized by low longitudinal conductance (0.1 - 0.2 mhos), suggesting low corrosivity. The remaining 15% of the area is

characterized by moderate (0.2 - 0.3 mhos), high (0.3 - 0.4 mhos), and very high (above 0.4 mhos) corrosivity.

Longitudinal Resistivity Map

The longitudinal resistivity map (Figure 10) reveals a pattern opposite to that of the longitudinal conductance map (Figure 9). The larger part of the study area, about 60%, especially the northwestern and southern sections, is characterized by very high longitudinal resistivity (above 200 Ωm), suggesting negligible corrosivity. About 15% of the area, especially in the central part, is characterized by high longitudinal resistivity (150 - 200 Ωm), suggesting low corrosivity. The remaining 25% of the area, mainly within the central part, is characterized by moderate (100 - 150 Ωm), low (50 - 100 Ωm), and very low (0 - 50 Ωm) longitudinal resistivity, corresponding to moderate, high, and very high corrosivity.

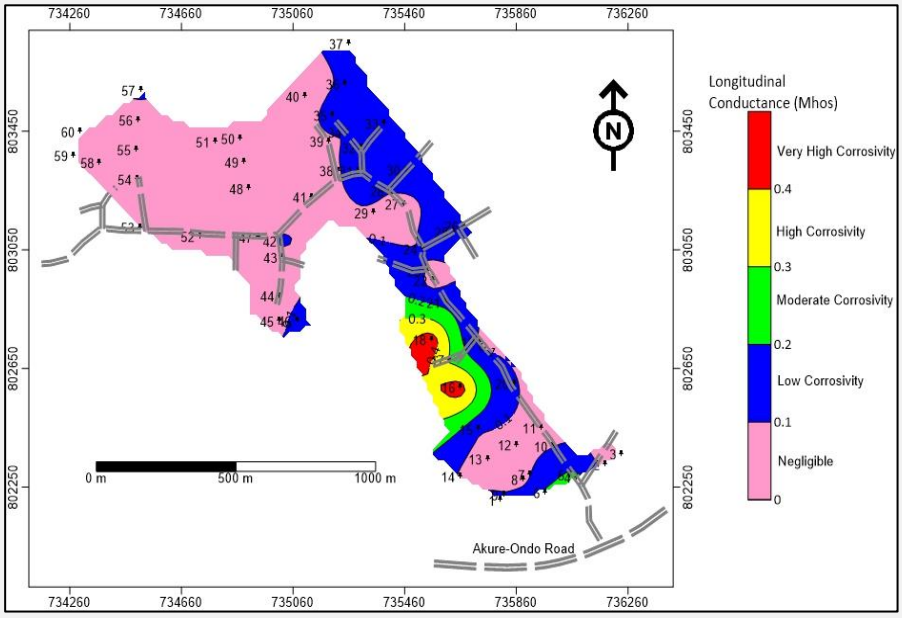

Figure 9. Longitudinal Conductance map of the study area.

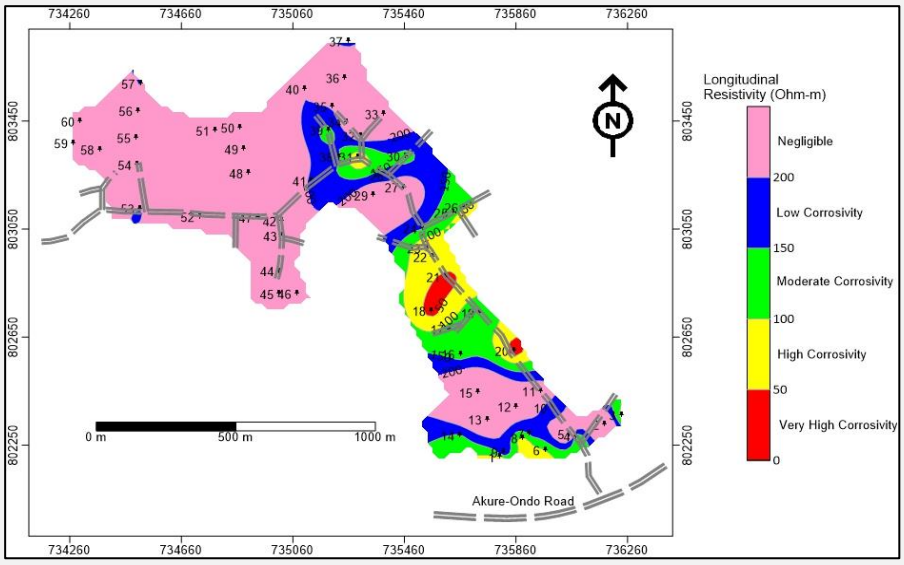

Figure 10. Longitudinal Resistivity map of the study area.

CONCLUSION

The 0.5 m depth slice map indicated that about 35% of the area has negligible to low corrosivity, while the 0.75 m depth slice map showed that 40% of the area has negligible to low corrosivity. At 1.0 m and 3.0 m depth surfaces, the area of negligible to low corrosivity increases to about 70% and 85%, respectively. The longitudinal conductance and longitudinal resistivity maps indicated that the area of negligible to low corrosivity is about 85% and 75%, respectively, which corroborates the depth slice resistivity maps of 1.0 and 3.0 m. The comparison of the depth slice maps reflects reducing corrosivity with depth within the shallow depth surfaces (0.5 to 3.0 m) of the study area.

This is in sharp contrast to the works of Adeyemo et al. (2018) and Adeyemo et al. (2019), where corrosivity was observed to be increasing with depth within the shallow subsurfaces. A major factor that might be responsible for this phenomenon is the presence of migmatite-gneiss-quartzite rocks in the area, which weather into sandy materials that have little affinity for water retention.

ACKNOWLEDGEMENT

The authors are grateful to the Department of Applied Geophysics, Federal University of Technology, Akure, Nigeria, for allowing us the use of the Omega Resistivity meter. We also express our thanks to the following friends and students from the same department who assisted in acquiring data for this work: Mr. Aruwaji Success I., Mr. Gade Adefolarinwa E., and Mr. Omole Boluwaji F.

REFERENCES

Adeoti, L., Ishola, K. S., & Adesanya, O. (2013). Subsurface Investigation Using Electrical Resistivity and Standard Penetration Test as Guide for Gas Pipeline Installation in Lekki Peninsula, Lagos. *European Journal of Geology and Environment (EJGE), 18*, 2791-2804.

Adeyemo, I. A. Olumilola, O. A., & Ibitomi, M. A. (2018). Geoelectrical and Geotechnical Investigations of Subsurface Corrosivity in Ondo State Industrial Layout, Akure, Southwestern Nigeria. *Ghana Mining* Journal, 18(1), 20-31. https://doi.org/10.4314/gm.v18i1.3

Adeyemo, I. A., Afolayan, A. I., Boluwade, B. S., & Alabi, S. K. (2023). Subsurface Geotechnical Competence Evaluation Using Geoelectric Sounding and Direct Cone Penetrometer Test at Plural Garden Estate, Ilaramokin Southwestern Nigeria. Indonesian Journal of Earth Sciences, 3(2), A618. https://doi.org/10.52562/injoes.2023.618

Adeyemo, I. A., Karounwi, S. A., & Oladeji, J. F. (2019). Geoelectric sounding and soil physicochemical tests for subsurface layers corrosivity investigations at Ilaramokin, near Akure, Southwestern Nigeria. *IOSR Journal of Applied Geology and Geophysics, 7*(6), 25-36.

Akintunde, O. A., & Ozebo, V. C. (2022). Integrated approach in evaluating subsurface corrosivity condition along a proposed gas pipe route at Obasanjo Farm, Obada Oko in Ogun State, Nigeria. *Arabian Journal of Geosciences, 15*(15), 1329. https://doi.org/10.1007/s12517-022-10539-y

Alagbe, O. A. (2018). 2D Geoelectrical Resistivity Imaging for the Assessment of Subsurface Soil Corrosivity Zones at a Proposed Filling Station Site in Akure Southwestern Nigeria. *International Advanced Research Journal in Science, Engineering and Technology, 5*(11), 58-73. https://doi.org/10.17148/IARJSET.2018.51112

Bayowa, O. G., & Adigun O. A. (2012) Evaluation of Subsoil Corrosivity Condition around a Sewage Pond using the Electrical Resistivity Method. A Case Study from the Basement Complex Terrain of Ile-Ife, Southwestern Nigeria. *Greener Journal of Physical Sciences, 2*(1), 10-15.

Bayowa, O. G., & Olayiwola, N. S. (2015). Electrical resistivity investigation for topsoil thickness, competence and corrosivity evaluation: a case study from Ladoke Akintola University of Technology, Ogbomoso, Nigeria. In *2nd international conference on geological and civil engineering. IPCBEE/ACSIT Press, Singapore* (Vol. 80, pp. 52-56).

Beavers, J. A., & Thompson, N. G. (2006). External corrosion of oil and natural gas pipelines. In *Corrosion: environments and industries* (pp. 1015-1025). ASM International.

Braford, L. J. (2000). Electrical resistivity testing. In *Nondestructive Testing Handbook, Second Edition: Infrared and Thermal Testing* (309-345). ASM International.

Dayal, R., Dayal, R., Singh, T. N., & Tewari, R. P. (1988). Studies on corrosion control of underground metallic structures: estimation of corrosion using different soil parameters. *Corrosion Science, 28*(3), 205-219.

Eyankware, M. O., & Umayah, S. O. (2022). 1D modeling of aquifer vulnerability and soil corrosivity within the sedimentary terrain in Southern Nigeria, using resistivity method. *World News of Natural Sciences, 41*, 33-50.

Gopal, M. (2010). Corrosion potential assessment. *The Geology of Part of South-Western Nigeria, Geological Survey of Nigeria*, 31-87.

Guma, D. K., Aondover, A. P., & Onoja, A. (2015). Soil corrosivity level of Kaduna metropolitan area using electrical resistivity method. *International Journal of Scientific and Engineering Research, 6*(2), 1408-1419.

Hussain, T., & Tarig, A. (2014). Study on corrosion rate of carbon steel in different soils. *Arabian Journal for Science and Engineering, 39*(12), 8165-8172.

Idornigie, A. I., Ehirim, N. C., & Anyiam, O. S. (2006). Determination of subsoil corrosivity zones in Akungba-Akoko area, Nigeria using electrical resistivity method. *Journal of Mining and Geology*, *42*(2), 115-124.
Iloeje, N. P. (1980). *A new Geography of Nigeria* (New Revised Edition). London, UK; Longman Group.
Keller, G. V., & Frischknecht F. C. (1966). *Electrical Methods in Geophysical Prospecting*. Pergamon Press, Oxford.
Koefoed, O. (1979). *Geosounding principles, 1, Resistivity Sounding Measurements*. Elsevier Scientific Publ. Co., Amsterdam-Oxford-New York.
Kosinski, W. K., & Kelly, W. E. (1981). Geoelectric soundings for predicting aquifer properties. *Groundwater*, *19*(2), 163-171. https://doi.org/10.1111/j.1745-6584.1981.tb03455.x
Najjaran, H., Khajehpour, M., Sharifi, M., & Aalami, M. (2004). Predicting corrosion rate of cast/ductile iron pipes in soil using fuzzy logic. *Corrosion Science*, *46*(5), 1115-1126.
Ngah, S. A., & Abam, T. K. S. (2014). Shallow resistivity measurements for subsoil corrosivity evaluation in Port Harcourt Metropolis, Nigeria. *International Journal of Science and Technology*, *3*(2), 85-91.
Oyawoye, M. O. (1964). The geology of the Nigerian Basement Complex-A survey of our present knowledge of them. *Journal of the Nigerian mining, geological and metallurgical Society*, *1*(2), 87-102.
Palmer, D. A. (1989). Corrosion of metals in soils. *Corrosion*, *45*(4), 297-303.
Picozzi, O. E., Lamb, S. E., & Frank, A. C. (1993). Evaluation of prediction methods for pile corrosion at the Buffalo Skyway. *New York State Department of Transportation, Technical Services Division*, *30*, 41-46.
Rahaman, M. A. (1988). Recent advances in the study of the basement complex of Nigeria. *Pre Cambrian geology of Nigeria*, 11-41.
Rahman, M. A. (1976). Review of the basement geology of southwestern Nigeria. In: Kogbe, CA (ed.), *Geology of Nigeria*. Elizabeth Publishing Co.
Rim-rukch, A. (2006). Effect of soil corrosivity on the performance of the cathodic protection systems. *International Journal of Electrochemical Science*, *1*(3), 123-131.
Romer, A. E., Bell, G. E. C., Duranceau, S. J., & Foreman, S. (2004*). External corrosion and corrosion control of buried water mains*. American Water Works Association.
Vander Velpen, B. P. A. (2004). WinRESIST version 1.0 resistivity depth sounding interpretation software. *M. Sc Research Project, ITC, Delf Netherland*.
Zohdy, A. A., Eaton, G. P., & Mabey, D. R. (1974). *Application of Surface Geophysics to Ground-water Investigations: Techniques of Water Resources Investigations of the United States Geological Survey: Book 2: Collection of Environmental Data: Chapter D1*. United States Department of the Interior.

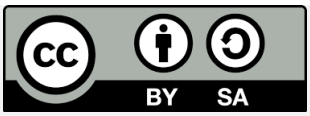

Copyright (c) 2024 by the authors. This work is licensed under a Creative Commons Attribution-ShareAlike 4.0 International License.